Presented at the 37th European PV Solar Energy Conference and Exhibition, 7-11 September 2020

DISPENSING TECHNOLOGY MEETS CIGS SUBSTRATES: FIRST IV-RESULTS WITH DISPENSED METAL GRID ON CIGS MINI-MODULES

K. Gensowski[1*], A. Jimenez[1], S. Tepner[1], M. Kuchler[2], M. Breitenbücher[2], T. Freund[3], P. Köder[3], J. Müller[3], B. Dimmler[3], M. Pospischil[1,2] and F. Clement[1]

[1]Fraunhofer Institute for Solar Energy Systems ISE, Heidenhofstraße 2, 79110 Freiburg im Breisgau, Germany
[2]HighLine Technology GmbH, Reichenbachstraße 18, 79117 Freiburg im Breisgau, Germany
[3]NICE Solar Energy GmbH, Alfred-Leikam-Straße 25, 74523 Schwäbisch Hall, Germany

*Corresponding author: Katharina Gensowski | Phone: +49 (0) 761/45 88-5197 | katharina.gensowski@ise.fraunhofer.de

ABSTRACT: For the first time, the parallel dispensing approach and the CIGS thin-film technology are combined to demonstrate metallization for thin-film PV with low temperature pastes. This article focuses on dispensing three different low temperature pastes through 35 µm and 25 µm nozzle openings, respectively, and applying them on 156 mm x 156 mm CIGS substrates. The screen printed metal grid acts as reference. The achieved contact resistivity values are below 5 mΩcm². The metal grid on the TCO layer of CIGS substrates obtains an increased short-circuit current density of Δj_{sc} = 1.1 mA·cm^{-2}, which corresponds to 3.5% current density gain compared to grid-free CIGS modules, and an increased module power of up to 4.6%. Additionally, the Fill Factor is positively affected by the metallization. Paste C shows a promising contact finger geometry with a core finger width of w_{core} = 25 µm ± 1 µm and an optical aspect ratio of AR_o= 0.46 ± 0.02. Following, the dispensing technology has been successfully applied on CIGS mini-modules as a future approach for realizing the metallization with a realistic perspective in terms of scalability for large module sizes.
Keywords: solar cell metallization, dispensing, low temperature paste, thin-film photovoltaics, CIGS

1 INTRODUCTION

Thin-film technologies, especially $Cu(In_{1-x}Ga_x)Se_2$ technology (CIGS), have a high efficiency potential which has been recently demonstrated by NICE Solar Energy GmbH, obtaining a new CIGS module record of 17.6% on a module area of 1.20 m x 0.60 m [1]. Solar Frontier achieved the CIGS cell record efficiency of 23.35% on a cell area of 1 cm² [2]. But nevertheless, the conventional silicon PV technologies dominate the global PV market [3, 4]. One reason for that is the efficiency gap between cell and module, which is up to 8% abs. between the CIGS cell record and commercial modules and only up to 4% abs. for crystalline silicon PV. Bermudez et al. present the metallization on the transparent conductive oxide (TCO) layer of CIGS substrates, so called hybrid modularization, as a promising solution to reduce the efficiency losses between CIGS cells and modules. Therefore, Bermudez et al. proposed inkjet as a potential printing technology [5].

The question arises why does the CIGS technology need an alternative printing technology compared to the well-known screen printing approach. To print the metal grid on the gigantic active printing area of the CIGS modules of approximately 60 cm x 120 cm, requires large screens which are limited in screen lifetime and also in fineness of the mesh. So, the screen optimization regarding a smaller finger geometry and lower paste consumption (fine-line screen printing), which is under constant development over the last years for silicon PV, is practicable limited for these huge screens [6, 7]. Following, the inhomogeneity of contact fingers caused by the mesh wires (mesh marks), in particular the deviation in finger height, becomes increasingly challenging to be further improved which results in a non-optimal silver consumption regarding electrical conductivity. Besides, such big screens tend to show significant distortion over their life cycle which complicates further industrial scaling. Another cost-intensive challenge of screen printing on CIGS modules is the required large silver paste volume which is exposed to the environment during the flooding procedure.

In this study, we present the parallel dispensing technology as an alternative approach to applying the metal grid on the CIGS substrates. Here, the high viscous paste is extruded through parallel arranged nozzle openings. Several publications show the successful demonstration of the dispensing technology for silicon PV applications [8–10]. Especially the non-limited upscaling of huge substrate areas, the closed paste reservoir and the homogeneous contact finger shape are beneficial properties of the parallel dispensing approach. The Fraunhofer spin-off HighLine Technology GmbH started in 2019 the commercialization of the multinozzle print head for dispensing [11].

This work presents the first dispensed contact fingers on 156 mm x 156 mm CIGS mini-modules by using TLM and IV measurements as characterization methods.

2 EXPERIMENTAL APPROACH

2.1 Applying metal grid by parallel dispensing and screen printing

Figure 1 summarizes all examined printing experiments conducted in this work. Each experimental group consists of five TLM substrates and ten mini-modules, respectively. Our project partner NICE Solar Energy GmbH fabricated 156 mm x 156 mm CIGS substrates that allow the application of production tools designed for silicon solar cells. Here, the different layers are deposited on 3 mm thick glass substrates. Seventeen cells with a cell width of 6.94 mm are positioned over an active module area of 137.43 cm². The mini-modules of

reference group 0 consist of cells with a width of 4.07 mm. The deposition of the different functional layers and its P1P2P3 scribing is well described in literature [12, 13]. In our case, the P1 scribing is carried out by laser, the P2 and P3 scribings are realized mechanically.

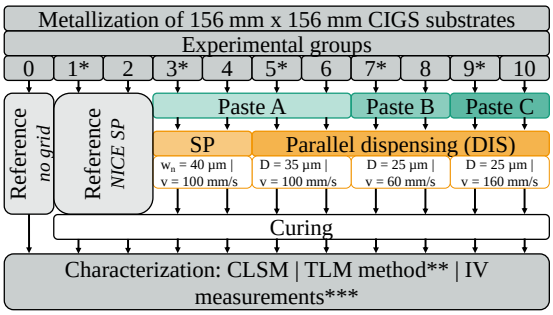

Figure 1: Experimental overview of the investigated screen printing (SP) and dispensing (DIS) experiments on CIGS substrates focuses on the application of three low temperature pastes by the dispensing approach. Paste A is extruded through D = 35 µm nozzle openings, pastes B and C are dispensed through D = 25 µm nozzle openings. For screen printing a screen with w_n = 40 µm screen openings is applied (group 3 and 4). The curing parameters were determined based on preliminary tests [14] and the substrates are characterized concerning their contact finger shapes and their electrical parameters (*CIGS TLM substrates, **characterization of CIGS TLM substrates, ***characterization of CIGS mini-modules).

The metal grids of reference groups 1 and 2 are screen printed, here a reference paste as well as reference process parameters of our project partner NICE Solar Energy GmbH are used. The screen printing experiments of group 3 and 4 are performed at a semi-automatic screen printer EKRA XH STS, the screen specification is 360 x 0.016 x 22.5° with an emulsion over screen of EOM = 15 µm. The screen openings are w_n = 40 µm, the applied squeegee speed is $v_{squeegee}$ = 100 mm/s.

Three different low temperature silver pastes A, B and C are evaluated for parallel dispensing. Paste A and B are commercially available screen printing pastes, paste C is a particularly adapted dispensing paste. The dispensing experiments are carried out at a dispensing platform from ASYS GmbH, Germany. The GECKO print head is integrated into this platform, here the nozzle plate with different nozzle openings can be flexibly installed depending on the paste properties [15]. Nozzle openings of D = 35 µm (finger pitch: 1.556 mm) are evaluated for the dispensing of paste A at a process velocity of v_{disp} = 100 mm/s. Paste B and paste C run through D = 25 µm nozzle openings (finger pitch: 1.194 mm). The applied dispensing speed is v_{disp} = 60 mm/s for paste B and v_{disp} = 160 mm/s for paste C. In this case, the dispensing gap between the nozzle plate and the CIGS substrate is set to 600 µm.

After applying the metal grids onto the TCO layer of the CIGS substrates, the samples are cured in a convection oven R0400FC from Essemtec AG, Switzerland. The pastes' specific curing parameters are evaluated in preliminary experiments presented in [14]. The chosen curing parameters are trade-offs between the lowest possible curing temperatures and durations that result in low contact resistivity. Paste A and paste B are cured at a temperature of T_c = 190°C, paste C is cured at a temperature of T_c = 180°C. The curing duration of all samples is t_c = 10 min. The CIGS substrates of group 1 and 2 are cured in a batch oven at T_c = 150°C for t_c = 5 min.

2.2 Characterization of printed metal grids on CIGS substrates

The contact finger geometry is determined by using the 3D confocal laser scanning microscope OLS4000 (CLSM) from Olympus. The microscope images are captured with a magnification of 50 and are analyzed by Fraunhofer internal software, here the finger width w, the finger height h and the cross section area A_{cross} are calculated [16]. The finger width is distinguished in core finger width w_{core} and shading finger width $w_{shading}$, there the shading finger width $w_{shading}$ is defined as the maximum shaded area in horizontal direction including any paste spreading. The core finger width w_{core} only includes the horizontal structure width that has a significant finger height [17]. Based on these data, the optical aspect ratio AR_o which is the ratio of the finger height to the shading finger width $w_{shading}$ and the electrical aspect ratio AR_{el} which is the ratio of the cross section A_{cross} to the shading finger width $w_{shading}$ are calculated.

The electrical characterization of the CIGS substrates is conducted by TLM Scan from pv-tools GmbH and h.a.l.m. flasher IV-tool at standard test conditions. The CIGS TLM samples are separated into 10 mm broad stripes to measure the contact resistivity and sheet resistance between the contact fingers. At least 150 measurements are conducted for each substrate. The CIGS mini-modules require the P1P2P3 scribing as well as contact stripes for IV measurements, which are executed with non-laminated modules at 1000 W/m².

3 RESULTS AND DISCUSSION

3.1 Analysis of contact finger geometry

The three investigated low temperature pastes show the typical homogeneous finger height profile by using the dispensing approach (see Figure 2). Compared to that, the screen printed contact fingers contain meshes marks which means a height deviation across the contact finger length. The reference group 1 has an average finger width of $w_{shading}$ = 54 µm ± 4 µm and an optical aspect ratio of AR_o = 0.21 ± 0.04 (AR_{el} = 0.13 ± 0.01). The samples of group 3 have a similar contact finger width of $w_{shading}$ = 55 µm ± 2 µm, but a higher optical aspect ratio of AR_o = 0.35 ± 0.03 (AR_{el} = 0.21 ± 0.02) than group 1 which may potentially result from different paste properties and screen specifications.

Figure 2 depicts microscope images and height images of dispensed contact fingers of pastes A, B and C. Dispensing paste A results in an average finger width of $w_{shading}$ = 46 µm ± 3 µm and an average core finger width of w_{core} = 36 µm ± 1 µm (group 5). The dispensed contact lines with paste B show similar geometric parameters. The average optical aspect ratio is AR_o = 0.35 ± 0.03. Paste C results in reduced core finger width of w_{core} = 25 µm ± 1 µm and an increased optical aspect ratio of AR_o = 0.46 ± 0.02. So, dispensed contact

fingers show improved contact finger geometries compared to screen printing resulting in a better electrical conductivity (more effective silver consumption). This increased contact finger homogeneity should allow the use of even wider cells in the CIGS modules than presented in this work. Consequently, the module voltage is reduced and the number of modules in one string can be increased resulting in lower balance of system costs. Reasons for the different paste performances of pastes A, B and C regarding process velocity and achieved contact finger geometry are not yet completely explicable.

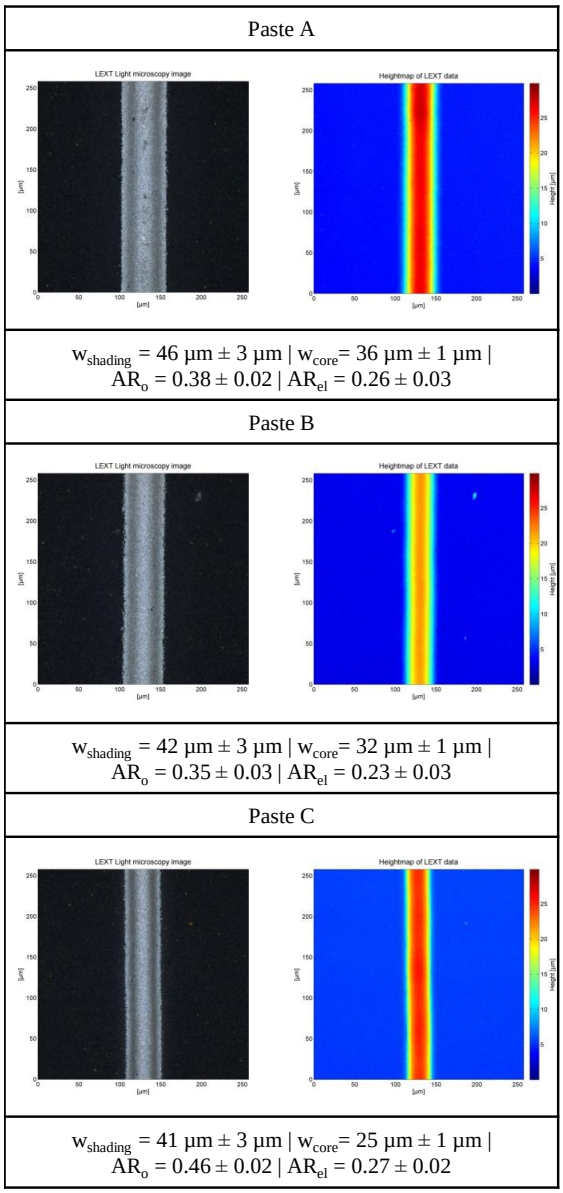

Figure 2: 3D confocal laser microscope images and height analysis of the dispensed contact fingers of low temperature pastes A, B and C [14].

3.2 Electrical characterization of CIGS substrates

The contact resistivity and sheet resistance values are depicted in Figure 3. Both, screen printed and dispensed contact fingers have average contact resistivities below 5 mΩcm² independent of the applied curing parameters. The average sheet resistance of all samples is in the range of $R_{sh,TLM}$ = 64 Ω/sq. ± 5 Ω/sq. (group 7) to $R_{sh,TLM}$ = 97 Ω/sq. ± 9 Ω/sq. (group 3), the reference samples of group 1 achieved a sheet resistance of $R_{sh,TLM}$ = 67 Ω/sq. ± 5 Ω/sq. by curing the samples at T_c = 150°C for t_c = 5 min. The CIGS TLM substrates of group 7 (paste B) reached the lowest contact resistivity of $\rho_{c,TLM}$ = 0.9 mΩcm² ± 0.7 mΩcm². Metal grids of paste C which are cured at T_c = 180°C for t_c = 10 min, also achieved a low contact resistivity of $\rho_{c,TLM}$ = 1.4 mΩcm² ± 1.0 mΩcm² and a sheet resistance of $R_{sh,TLM}$ = 64 Ω/sq. ± 6 Ω/sq.. A clear tendency regarding curing conditions or contact finger geometries is not evident for the TLM results. Further experimental studies are required to get a deeper understanding of the impact parameters of the contact formation.

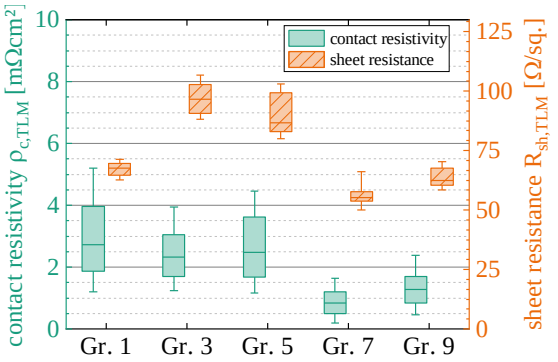

Figure 3: Contact resistivity $\rho_{c,TLM}$ and sheet resistance $R_{sh,TLM}$ results measured by TLM Scan. Each group consists of five CIGS TLM substrates, at least 150 measurements were carried out per substrate.

The considerable advantage of applying a metal grid onto the TCO layer of CIGS modules is visible in the short-circuit current values in Figure 4. The metallization and the possibility to use wider cells increase the short-circuit current significantly. The grid-free CIGS mini-modules with cell widths of 4.07 mm have in average a short-circuit current of J_{sc} = 143 mA ± 1 mA (j_{sc} = 31.1 mA·cm^{-2} ± 0.1 mA·cm^{-2}) compared to metallized CIGS mini-modules which show short-circuit current values between J_{sc} = 256 mA ± 1 mA (j_{sc} = 31.7 mA·cm^{-2} ± 0.3 mA·cm^{-2}) and J_{sc} = 260 mA ± 1 mA (j_{sc} = 32.2 mA·cm^{-2} ± 0.1 mA·cm^{-2}). Consequently, the short-circuit current has been increased up to ΔJ_{sc} = 117 mA, the short-circuit current density up to Δj_{sc} = 1.1 mA·cm^{-2}. At the same time, the open-circuit voltage values present room for improving. The grid-free CIGS mini-modules have an open-circuit voltage of V_{oc} = 20.05 V ± 0.07 V, all CIGS mini-modules with metal grid show open-circuit voltage values in the range of V_{oc} = 11.06 V ± 0.06 V to V_{oc} = 11.78 V ± 0.06 V. CIGS mini-modules of group 2 are cured at the lowest curing temperature of T_c = 150°C by achieving the highest open-circuit voltage of V_{oc} = 11.78 V ± 0.06 V. Applying the low temperature paste C on CIGS mini-modules by dispensing results in an average open-circuit voltage of V_{oc} = 11.43 V ± 0.15 V. One possible explanation for these results might be that the chosen curing parameters affect the CIGS layer's thermal damages or diffusion processes in the cadmium sulfide layer. In this experiment, the different contact finger shapes do not show a high impact on the IV results because the low as well as high optical aspect ratios and also different core finger widths partly result in similar

open-circuit voltages. Depending on the used screen layout and the nozzle openings, the finger pitches differ which results in different finger numbers per area. In literature, simulation results show the optimal finger number per cell area [18]. This impact regarding the IV results should be carried out in further studies. Besides, low temperature silver pastes that already form low contact resistivity contacts are necessary to prevent the remarkable decrease of the open-circuit voltage.

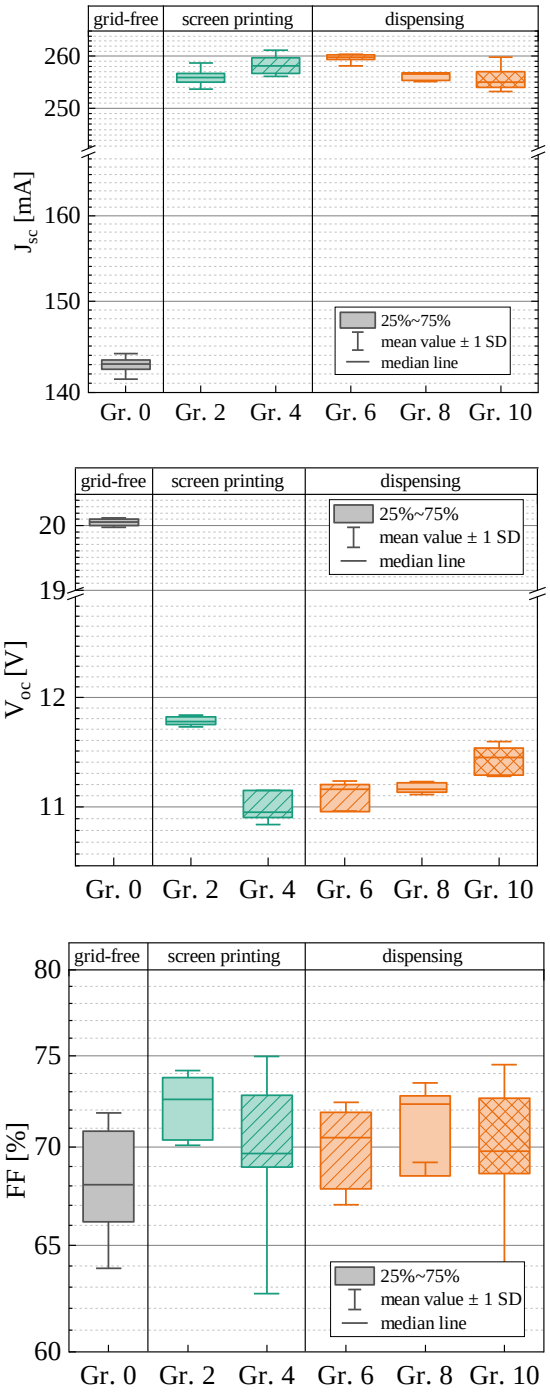

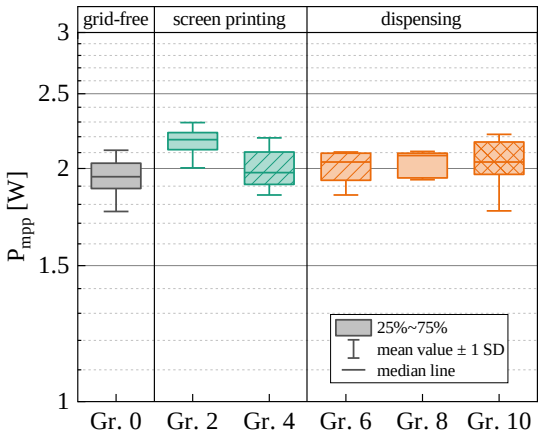

Figure 4: IV results of 156 mm x 156 mm CIGS mini-modules measured by h.a.l.m. flasher IV-tool at standard test conditions. The J_{sc}-, V_{oc}-, FF- and P_{mpp}-values are plotted. The cell width of samples of group 0 is 4.07 mm, all other CIGS mini-modules have cells with a width of 6.94 mm.

Further positive effects of applying metal grid on the TCO layer are evident in the Fill Factor values and also in the module power. Both parameters have been improved. The Fill Factors of group 2 to 10 vary between FF = 68.7% ± 5.6% and FF = 72.1% ± 2.0% compared to the grid-free CIGS mini-module of group 0 with an average Fill Factor of FF = 67.9% ± 3.9%. Besides, the module power P_{mpp} has been increased up to ΔP_{mmp} = 0.22 W, the non-metallized CIGS mini-modules present an average module power of P_{mpp} = 1.95 W ± 0.12 W.

All depicted IV results in Figure 4 are determined before lightsoaking. Subsequently, the CIGS mini-modules are lightsoaked for 48 hours and are characterized again by h.a.l.m. flasher IV-tool at standard test conditions. The lightsoaking obtains a slightly increased open-circuit voltage of up to ΔV_{oc} = 0.16 V, the other IV parameters remain similar to those before lightsoaking.

4 SUMMARY AND OUTLOOK

In this study, we demonstrated the advantages of applying a metal grid on the TCO layer of CIGS mini-modules by showing a gain in module performance. Further, we presented the parallel dispensing approach as an alternative metallization technology for applying low temperature pastes. A screen printing approach as applied for the metallization of Silicon Heterojunction solar cells serves as reference. Along with a substantial improved homogeneity of dispensed contact fingers, the beneficial advantages of the parallel dispensing compared to screen printing on huge CIGS modules are the non-limited upscaling on large substrate areas as well as the extremely reduced required silver paste volume in a closed reservoir. Three different, commercially available low temperature silver pastes are evaluated in this experiment by showing advantages in electrical parameters compared to grid-free CIGS mini-modules. The contact resistivity of all samples is below 5 mΩcm². The metal grid on CIGS substrates allows the use of broader cell widths of 6.94 mm, thus, the dead area of

CIGS modules could be minimized and the short-circuit current density gains in Δj_{sc} = 1.1 mA·cm^{-2}. Also, the Fill Factor (ΔFF = 4.3%) and the module power (ΔP_{mpp} = 0.22 W) of metallized CIGS mini-modules have improved values compared to grid-free samples. Paste C achieved a promising contact finger geometry regarding shading effects, the average core finger width is w_{core} = 25 µm ± 1 µm and the optical aspect ratio is AR_o = 0.46 ± 0.02. The homogenous contact finger height of dispensed structures allows a more effective silver consumption regarding the electrical conductivity and should allow the use of broader cell widths in the CIGS modules compared to screen printed metal grids. This possible balance of system cost advantage is examined in the future. The combination of the dispensing approach and CIGS technology was successfully demonstrated.

Further studies require dispensable low temperature pastes that form contacts with low contact resistivity values for curing temperatures below 180°C to prevent the significant losses in open-circuit voltage. The parallel dispensing process needs to be demonstrated on large module sizes, using the multinozzle print head of HighLine Technology GmbH as the next step.

5 ACKNOWLEDGEMENT

The authors would like to thank all co-workers at Fraunhofer Institute Solar Energy Systems ISE, at NICE Solar Energy GmbH as well as at HighLine Technology GmbH for supporting our work. This work was financed by the German Federal Ministry for Economic Affairs and Energy with the project “Altura”, contract number 03EE1006C.

6 REFERENCES

[1] S. Enkhardt, *Manz-Joint-Venture Nice Solar Energy vermeldet Wirkungsgradrekord von 17,6 Prozent für CIGS-Module.* [Online]. Available: https://www.pv-magazine.de/2019/12/04/manz-joint-venture-nice-solar-energy-vermeldet-wirkungsgradrekord-von-176-prozent-fuer-cigs-module/ (accessed: Jan. 22 2020).

[2] S. Yoshida, *Solar Frontier Achieves World Record Thin-Film Solar Cell Efficiency of 23.35%.* [Online]. Available: http://www.solar-frontier.com/eng/news/2019/0117_press.html (accessed: Jun. 22 2020).

[3] *CIGS White Paper 2019.* [Online]. Available: https://cigs-pv.net/wortpresse/wp-content/uploads/2019/04/CIGS_White_Paper_2019_online.pdf (accessed: Feb. 3 2020).

[4] VDMA Photovoltaics Equipment, “International Technology Roadmap for Photovoltaics (ITRPV): Eleventh Edition,” 2020.

[5] V. Bermudez and A. Perez-Rodriguez, “Understanding the cell-to-module efficiency gap in Cu(In,Ga)(S,Se)2 photovoltaics scale-up,” *Nat Energy*, vol. 3, no. 6, pp. 466–475, 2018, doi: 10.1038/s41560-018-0177-1.

[6] S. Tepner, N. Wengenmeyr, L. Ney, M. Linse, M. Pospischil, and F. Clement, “Improving Wall Slip Behavior of Silver Pastes on Screen Emulsions for Fine Line Screen Printing,” *Solar Energy Materials and Solar Cells*, vol. 200, p. 109969, 2019, doi: 10.1016/j.solmat.2019.109969.

[7] F. Clement *et al.*, “"Project FINALE"-screen and screen printing process development for ultra-fine-line contacts below 20 µm finger width,” *Proc. 36th Eur. Photovolt. Sol. Energy Conf. Exhib.*, vol. 2019, pp. 255–258, doi: 10.4229/EUPVSEC20192019-2DO.5.1.

[8] M. Pospischil *et al.*, “Applications of parallel dispensing in PV metallization,” *AIP Conference Proceedings, vol. 2156:1*, p. 20005, 2019, doi: 10.1063/1.5125870.

[9] M. Pospischil, “A parallel dispensing system for an improved front surface metallization of silicon solar cells,” Dissertation, Fraunhofer-Institut für Solare Energiesysteme.

[10] K. Gensowski *et al.*, “Conductive highly filled suspensions for an electrochemical dispensing approach to pattern full-area thin metal layers by physical vapour deposition,” *Scientific reports*, 2020, doi: 10.1038/s41598-020-64105-1.

[11] HighLine Technology GmbH. [Online]. Available: https://highline-technology.com/ (accessed: Aug. 5 2020).

[12] N. Mufti *et al.*, “Review of CIGS-based solar cells manufacturing by structural engineering,” *Solar Energy*, vol. 207, pp. 1146–1157, 2020, doi: 10.1016/j.solener.2020.07.065.

[13] V. Petrova-Koch, R. Hezel, and A. Goetzberger, Eds., *High-Efficient Low-Cost Photovoltaics: Recent Developments*: Springer, 2019.

[14] K. Gensowski *et al.*, “CIGS Mini-Modules with Dispensed Metallization on TCO layer,” submitted for publication.

[15] M. Pospischil *et al.*, “Process Development for a High-throughput Fine Line Metallization Approach Based on Dispensing Technology,” *Energy Procedia*, vol. 43, pp. 111–116, 2013, doi: 10.1016/j.egypro.2014.02.001.

[16] T. Strauch, M. Demant, A. Lorenz, J. Haunschild, and S. Rein, “Two image processing tools to analyse alkaline texture and contact finger geometry in microscope images,” *Proc. 29th Eur. Photovolt. Sol. Energy Conf. Exhib*, pp. 1132–1137, 2014, doi: 10.4229/EUPVSEC20142014-2BV.8.12.

[17] S. Tepner, N. Wengenmeyr, M. Linse, A. Lorenz, M. Pospischil, and F. Clement, “The link between Ag-paste rheology and screen printed solar cell metallization,” *Adv. Mater. Technolog.*, 2020, doi: 10.1002/admt.202000654.

[18] N. Bednar, N. Severino, and N. Adamovic, “Front grid optimization of Cu(In,Ga)Se 2 solar cells using hybrid modeling approach,” *Journal of Renewable and Sustainable Energy*, vol. 7, no. 1, p. 11201, 2015, doi: 10.1063/1.4908064.